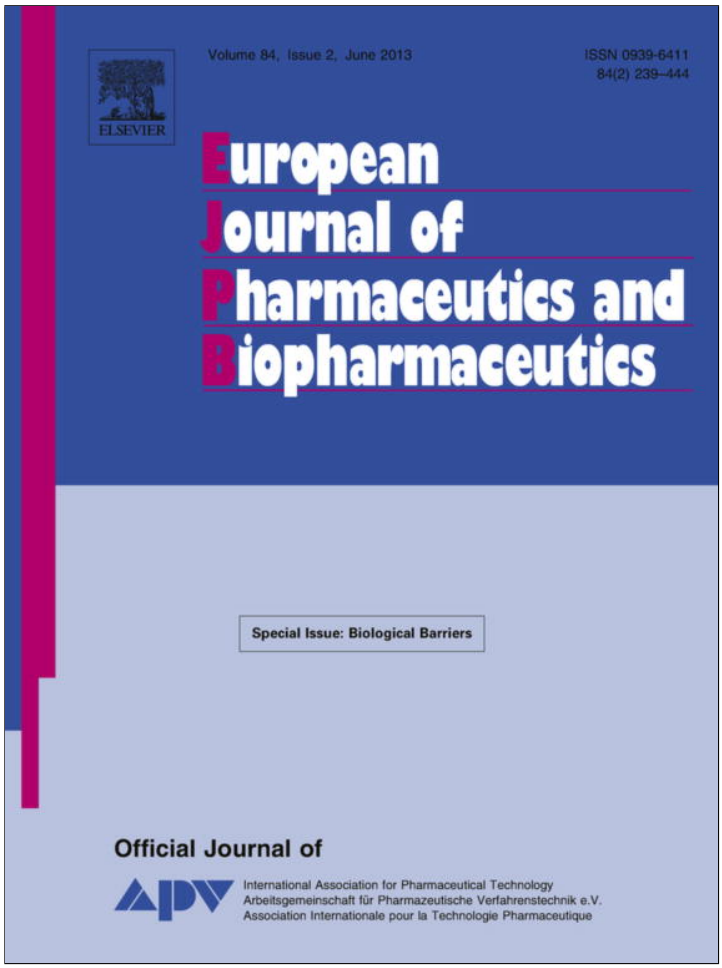

European Journal of Pharmaceutics and Biopharmaceutics 84 (2013) 355–364

Contents lists available at SciVerse ScienceDirect

European Journal of Pharmaceutics and Biopharmaceutics

journal homepage: www.elsevier.com/locate/ejpb

Research paper

Controlled intra- and transdermal protein delivery using a minimally invasive Erbium:YAG fractional laser ablation technology

Y.G. Bachhav [a,1], A. Heinrich [b], Y.N. Kalia [a,*]

[a] School of Pharmaceutical Sciences, University of Geneva, Geneva, Switzerland
[b] Pantec Biosolutions AG, Ruggell, Liechtenstein

ARTICLE INFO

Article history:
Available online 30 November 2012

Keywords:
Transdermal drug delivery
Fractional laser ablation
Protein delivery
Erbium:YAG
Follicle stimulating hormone (FSH)
Human growth hormone

ABSTRACT

The aim of the study was (i) to investigate the feasibility of using fractional laser ablation to create micropore arrays in order to deliver proteins into and across the skin and (ii) to demonstrate how transport rates could be controlled by variation of poration and formulation conditions. Four proteins with very different structures and properties were investigated – equine heart cytochrome c (Cyt c; 12.4 kDa), recombinant human growth hormone expressed in *Escherichia coli* (hGH; 22 kDa), urinary follicle stimulating hormone (FSH; 30 kDa) and FITC-labelled bovine serum albumin (FITC-BSA; 70 kDa). The transport experiments were performed using a scanning Er:YAG diode pumped laser (P.L.E.A.S.E.®; Precise Laser Epidermal System). The distribution of FITC-BSA in the micropores following P.L.E.A.S.E.® poration was visualised by using confocal laser scanning microscopy (CLSM). Porcine skin was used for the device parameter and CLSM studies; its validity as a model was confirmed by subsequent comparison with transport of Cyt c and FITC-BSA across P.L.E.A.S.E.® porated human skin. No protein transport (deposition or permeation) was observed across intact skin; however, P.L.E.A.S.E.® poration enabled total delivery after 24 h of 48.2 ± 8.9, 8.1 ± 4.2, 0.2 ± 0.1 and 273.3 ± 30.6 μg/cm^2 for Cyt c, hGH, FSH and FITC-BSA, respectively, using 900 pores/135.9 cm^2. Calculation of permeability coefficients showed that there was no linear dependence of transport on molecular weight ((1.6 ± 0.3), (0.1 ± 0.05), (0.08 ± 0.03) and (0.9 ± 0.1) × 10^{-3} cm/h, for Cyt c, hGH, FSH and FITC-BSA, respectively); indeed, a U-shaped curve was observed. This suggested that molecular weight was not a sufficiently sensitive descriptor and that transport was more likely to be determined by the surface properties of the respective proteins since these would govern interactions with the local microenvironment. Increasing pore density (i.e. the number of micropores per unit area) had a statistically significant effect on the cumulative permeation of both Cyt c (at 100, 150, 300 and 600 pores/cm^2, permeation was 11.2 ± 2.4, 15.3 ± 11.8, 33.8 ± 10.5 and 51.2 ± 15.8 4 μg/cm^2, respectively) and FITC-BSA (at 50, 100, 150 and 300 pores/cm^2, it was 58.5 ± 15.3, 132.6 ± 40.0, 192.7 ± 24.4, 293.3 ± 76.5 μg/cm^2, respectively). Linear relationships were established in both cases. However, only the delivery of FITC-BSA was improved upon increasing fluence (53.3 ± 22.5, 293.3 ± 76.5, 329.6 ± 11.5 and 222.1 ± 29.4 μg/cm^2 at 22.65, 45.3, 90.6 and 135.9 J/cm^2, respectively). The impact of fluence – and hence pore depth – on transport will depend on the relative diffusivities of the protein in the micropore and in the 'bulk' epidermis/dermis. Experiments with Cyt c and FSH confirmed that delivery was dependent upon concentration, and it was shown that therapeutic delivery of the latter was feasible. Cumulative permeation of Cyt c and FITC-BSA was also shown to be statistically equivalent across porcine and human skin. In conclusion, it was demonstrated that laser microporation enabled protein delivery into and across the skin and that this could be modulated via the poration parameters and was also dependent upon the concentration gradient in the pore. However, the role of protein physicochemical properties and their influence on transport rates remains to be elucidated and will be explored in future studies.

1. Introduction

Pharmacological potency, biological specificity and a concomitant decrease in the risk of side-effects make peptides and proteins extremely interesting leads for the development of new therapeutics [1]. Their physicochemical properties and stability requirements mean that they are almost always administered

* Corresponding author. School of Pharmaceutical Sciences, University of Geneva, 30 Quai Ernest Ansermet, 1211 Geneva, Switzerland, Tel.: +41 (0) 22 379 3355; fax: +41 (0) 22 379 3360.
E-mail address: Yogi.kalia@unige.ch (Y.N. Kalia).
[1] Present address: Debiopharm SA, espace "après-demain", EPFL, Quartier de l'innovation, Bâtiment G, 1015 Lausanne, Switzerland.

0939-6411/$ - see front matter © 2012 Elsevier B.V. All rights reserved.
http://dx.doi.org/10.1016/j.ejpb.2012.11.018

parenterally – most frequently by subcutaneous or intramuscular injection [2]. Although tolerable, this is non-ideal and new approaches to the controlled intra-epidermal, intra-dermal or transdermal delivery of these agents may open the door to alternative, less invasive strategies for effective targeted local delivery or systemic administration of 'biotech' therapeutics.

However, the stratum corneum – the uppermost layer of the epidermis – represents a formidable barrier against the transport of even small hydrophilic molecules into the body [3]. Hence, it is unrealistic to envisage that passive diffusion of peptides and proteins across intact and healthy skin will be sufficient to enable therapeutic amounts to be delivered in reasonable timeframes. As a result, several 'minimally invasive' techniques have been developed to reversibly compromise skin barrier function and so facilitate molecular transport while provoking minimal irritation at the application site [4,5]. These methods involve the creation of transport channels in the skin either by mechanical perforation (e.g. via the use of microneedles) or by the application of physical energy (e.g. radiofrequency) [6–8].

The P.L.E.A.S.E.® (Precise Laser Epidermal System) device contains a scanning Er:YAG laser that emits short duration pulses of radiation at 2.94 μm, a principal excitation wavelength for water molecules [9–17]. Application of laser energy to the skin results in their excitation and subsequent explosive evaporation from the epidermis, which in turn leads to the formation of micropores. Since the duration of the energy pulse is shorter than the thermal relaxation time of water, there is negligible heat transfer – and hence thermal damage – to the surrounding tissues. In contrast to laser devices that have frequently been used in earlier studies to enhance drug delivery with large beam spot diameters (3–7 mm) and which removed appreciable areas of contiguous skin [18–21]; the P.L.E.A.S.E.® device is a scanning fractional laser ablation system with a much narrower beam that creates smaller pores (typical diameter 150–200 μm) [9,10]. The major advantage of this 'fractional ablation' of the skin is that the micropores are surrounded by healthy tissue which facilitates skin recovery; typically, only 5–15% of the skin surface is removed [22–24]. A significant advantage of the P.L.E.A.S.E.® technology is the control afforded over delivery kinetics by modulation of the number of micropores created per cm^2 (i.e. pore density) and their depth. The latter is controlled by varying the amount of laser energy applied per unit area (or fluence; J/cm^2) to create each micropore [10,12–15]. Furthermore, since it is a scanning system, the full energy of the laser beam is applied to create each micropore in the array instead of the need for a fractionation of the beam [25]. Previous studies with the P.L.E.A.S.E.® system have demonstrated the controlled delivery of lidocaine, diclofenac and prednisone across porcine and human skin [10,12,14]. Preliminary studies have also shown the feasibility of using this technique to deliver a structurally intact peptide (exenatide [13]) and a protein (cytochrome c [11]). More recently, the first report into the use of fractional laser ablation for the 'needle-less' controlled delivery of structurally intact and biologically active therapeutic antibodies into and across the skin has also been published [15]. However, to-date, there is no information concerning the effect of permeant physicochemical properties – of low and (obviously) high molecular weight species – on transport through laser porated skin. The aim of this study was to investigate the effect of P.L.E.A.S.E.® poration and formulation parameters on the delivery kinetics of four proteins of different sizes and molecular properties through laser treated skin: namely, equine heart cytochrome c (Cyt c; 12.4 kDa) [26], recombinant human growth hormone expressed in *Escherichia coli* (rhGH; 22 kDa) [27], urinary follicle stimulating hormone – a post-translationally modified heterodimer, where two Asn residues are glycosylated in both the alpha and beta chains (FSH; 30 kDa) [28] and FITC-labelled bovine serum albumin (FITC-BSA; 70 kDa) [29] (Fig. 1). There is an approximately 6-fold difference in molecular weight, and the proteins have different secondary structure elements and as mentioned above, FSH is also glycosylated; these are all factors which may influence transport or affect the types of interactions with the transport pathway.

The specific objectives of the present investigation were (i) to demonstrate feasibility of protein delivery and to identify any common trends and (ii) to investigate the effect of micropore density (i.e. the number of micropores per cm^2 and hence the fractional ablated area) and of fluence (and hence pore depth) on protein transport through the skin and how these parameters could be used to control delivery, and (iii) to study the influence of protein concentration on transport. In addition, the presence of the FITC label conjugated to BSA meant that it could be visualised in the skin by confocal laser scanning microscopy.

2. Materials and methods

2.1. Chemicals

Equine heart cytochrome c, FITC and FITC-BSA were purchased from Fluka (Buchs, Switzerland). Follicle stimulating hormone

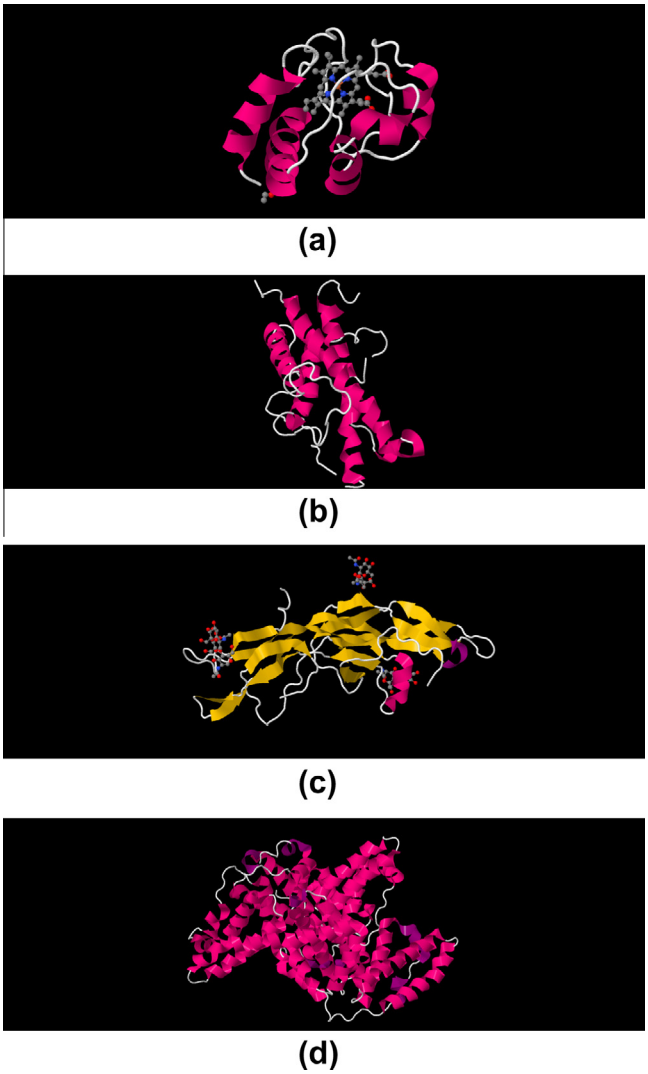

Fig. 1. Three dimensional representations of (a) Cyt c (using 1HRC.pdb), (b) hGH (using 1HGU.pdb), (c) FSH (using 1FL7.pdb) and (d) BSA (using 3VO3.pdb) illustrating the different secondary structure elements. (For interpretation of the references to colour in this figure legend, the reader is referred to the web version of this article.)

(FSH) (Fostimon®, Institut Biochmique SA (IBSA) was generously supplied as a gift. Acetonitrile (Chromasolv HPLC) gradient grade was purchased from VWR (Nyon, Switzerland). Trifluoroacetic acid was purchased from Acros Organics (Chemie Brunschwig, Basel, Switzerland). ELISA kits to quantify hGH (DSL-10-4700 ACTIVE®) and FSH (DRG FSH ELISA EIA-128) were purchased from DSL Inc. (Texas, USA) and DRG Diagnostics (Germany), respectively. Millex filters (0.45 μm PVDF) were purchased from Millipore, (Bedford, MA, USA). Deionised water (resistivity > 18 MΩ cm; Milli-Q Water Purification System (Millipore; Bedford, USA)) was used to prepare all solutions unless specified otherwise.

2.2. Skin

Porcine ears were supplied by a local abattoir (CARRE; Rolle, Switzerland) shortly after sacrifice. After cleaning under cold running water, the whole skin was carefully removed from the outer region of the ear and separated from the underlying cartilage with a scalpel. Skin samples were wrapped in Parafilm™ and maintained at −20 °C for no longer than a period of 2 months before use. Protein transport across laser porated skin was investigated using both dermatomed (0.75 mm; obtained with an air-dermatome (Zimmer; Etupes, France) and full thickness (typically, 1.0–1.5 mm) porcine ear skins. Human skin samples were collected immediately after abdominoplasty from the Department of Plastic, Aesthetic and Reconstructive Surgery, Geneva University Hospital (Geneva, Switzerland), fatty tissue was removed and the skin was wrapped in Parafilm™ before storage at −20 °C for a maximum period of 3 days. The study was approved by the Central Committee for Ethics in Research (CER: 08-150 (NAC08-051); Geneva University Hospital).

2.3. Experimental protocol for protein delivery studies

Skin samples (dermatomed and full thickness porcine and human skins) were equilibrated in 0.9% NaCl for 30 min before microporation using the P.L.E.A.S.E.® device. After removing surface moisture, skin samples were mounted in a custom designed assembly and placed at the laser focal length to create the microchannels. The microporation parameters, that is, number of micropores and fluence (number of energy pulses applied to create each pore), were fixed by the user. Skin samples (either intact (untreated) or P.L.E.A.S.E.® porated) were mounted in Franz diffusion cells ($A = 3.0 \pm 0.1$ cm^2), and silicone grease was applied to ensure a water tight seal. The receptor compartment (volume 9–10 ml) was filled with PBS (pH 7.4) for Cyt c, Tris buffer (pH 7.4) for FITC-BSA, and 25 mM HEPES/133 mM NaCl buffer (pH 7.4) for FSH and hGH. After equilibration, the formulations (details mentioned below) were placed in the donor compartment. The receptor phase was stirred at room temperature throughout the experiment, 0.4 ml of receptor phase was withdrawn at 3, 6 and 24 h, and each aliquot was replaced with an equivalent volume of fresh buffer. At the end of the permeation experiment (24 h), the diffusion cells were dismantled and the skin surface washed in cold running water to remove any residual donor formulation. The skin samples were then cut into small pieces and soaked in 10 ml of the respective receptor phase (except for Cyt c, where mobile phase was used as an extraction medium) for 4 h under constant agitation at ambient temperature. Samples were filtered through 0.45 μm PVDF membrane 4filters prior to analysis to determine the amount of protein retained in the skin.

The following transport studies were performed.

2.3.1. Evaluation of the feasibility of protein delivery

Skin transport of Cyt c (1 ml of 1 mg/ml), hGH (1.5 ml of 3.33 mg/ml), FSH (1 ml of 25 μg/ml) and FITC-BSA (1 ml of 10 mg/ml) was investigated using dermatomed porcine skin at 0 and 300 pores/cm^2 (fractional ablated area (FAA) of 7.22%) at a fluence of 135 J/cm^2.

2.3.2. Effect of pore density – fractional ablated area

The effect of increasing the number of micropores on skin transport of Cyt c (from 1 ml of 1 mg/ml) and FITC-BSA (from 1 ml of 10 mg/ml) was investigated by varying the pore density at a fixed fluence. Pore densities of 100, 150, 300 and 600 pores/cm^2 (corresponding to 300, 450, 900 and 1800 pores in an area of 3 cm^2) at 22.65 J/cm^2 and 50, 100, 150 and 300 pores/cm^2 at 45.3 J/cm^2 were used for Cyt c and FITC-BSA, respectively.

2.3.3. Effect of fluence – pore depth

The effect of increasing fluence and thereby pore depth on skin transport of Cyt c (from 1 ml of 1 mg/ml) and FITC-BSA (from 1 ml of 10 mg/ml) was studied by applying energy pulses at the following fluences 22.65, 45.3 90.6 and 135.9 J/cm^2; pore density was fixed at 300 pores/cm^2.

2.3.4. Effect of concentration

The influence of protein concentration in the donor compartment on transport across P.L.E.A.S.E.® porated skin was studied by comparing delivery of (i) Cyt c at 1 and 5 mg/ml and (ii) FSH at 25, 165, 330 and 666 μg/ml. In both cases, the pore density was 300 pores/cm^2 (or 900 pores in 3 cm^2) and the fluence was fixed at 135 J/cm^2.

2.3.5. Comparison of transport kinetics across porcine and human skin

Skin transport of Cyt c (1 mg/ml) and FITC-BSA (10 mg/ml) across full thickness human skin samples porated with 300 pores/cm^2 (or 900 pores in 3 cm^2) at a fluence of 135.9 J/cm^2 was followed over 24 h.

2.4. Analytical methods

2.4.1. Cytochrome c

The amount of Cyt c permeated across and deposited within the skin was quantified by using a validated HPLC method developed in-house (using a Dionex Ultimate 3000 system equipped with an AD25 UV absorbance detector (Dionex; Olten, Switzerland)) [10]. Briefly, isocratic separation was performed using a 150 × 4.6 mm column packed with 5 μm C4 silica reverse-phase particles (Phenomenex; Paris, France) thermostatted at 35 °C. The mobile phase was a 41: 59 mixture of organic phase A (0.1% TFA in a 90:10 mixture of MeCN/H_2O) and an aqueous phase B (0.1% TFA in H_2O). The protein was detected by its absorbance at 400 nm, and the injection volume was 75 μl. The method was linear over the concentration range of 2.5–25 μg/ml. The LOD and LOQ were 0.76 and 2.3 μg/ml, respectively.

2.4.2. FITC-BSA

Skin permeation and deposition of FITC-labelled BSA were quantified by using a Fluoromax®-2 spectrophotometer (SPEX instruments SA Inc., UK). Measurements were made at 25 °C using a thermostatted cuvette holder. The samples were excited at 496 nm, and the emission was monitored between 500 and 650 nm using bandpasses of 1.0 nm (excitation) and 2.0 nm (emission), respectively. The method was linear over the concentration range of 0.5–100 μg/ml. The LOD and LOQ were 0.06 and 0.2 μg/ml, respectively.

The absence of free FITC was confirmed by comparing mass spectra of standard solutions of FITC, FITC-BSA and samples (taken from the receiver compartment post-permeation and after skin extraction) and samples of skin 'blank' (i.e. receptor medium 24 h post-poration but without application of FITC-BSA). The samples were analysed using a Turbo Ionspray (API 150 EX, Applied

Biosciences). Mass spectrometric analysis (MALDI-TOF; Axima CFR+(Shimadzu)) was performed for standards and skin transport samples of FITC-BSA according to protocols set-up by the High Resolution MS Platform, University of Geneva.

2.4.3. Follicle stimulating hormone

FSH permeation and deposition within the skin were quantified by ELISA (DRG FSH ELISA EIA-1288; DRG Instruments GmbH, Germany). The FSH test was based on a two step sandwich type immunoassay. Briefly, in order to determine the FSH content in the skin transport samples, test samples and standards were incubated in the microtitration wells which were coated with anti-FSH antibody. After incubation (30 min) and washing (5X), the wells were treated with another anti-FSH detection antibody labelled with the enzyme horseradish peroxidase (HRP). After a second incubation (30 min) and washing step (5X), the wells were incubated with the substrate tetramethylbenzidine (TMB). Finally, the reaction was stopped by using an acidic stopping solution. The degree of enzymatic turnover of the substrate was determined by dual wavelength absorbance measurement at 450 and 620 nm (Sunrise™; Tecan, Switzerland). The absorbance measured was directly proportional to the concentration of FSH. The method was linear between 0.15 and 15 ng/ml. The LOD and LOQ were 0.06 and 0.2 ng/ml, respectively.

2.4.4. Human growth hormone

The amount of hGH permeated across skin was also quantified by ELISA (DSL-10–1900; Diagnostic Systems Laboratories, Inc., TX USA). The test involved use of a sheep anti-hGH antibody for solid phase immobilisation (microtitre wells) and a mouse monoclonal anti-hGH antibody in the antibody-enzyme (horseradish peroxidase) conjugate solution. The test samples (and the standards) were allowed to react simultaneously with the antibodies, resulting in hGH being sandwiched between the solid phase and enzyme-linked antibodies. After incubation for 45 min at room temperature, the microwells were washed with water (5X) to remove unbound labelled antibodies. A solution of tetramethylbenzidine (TMB) was then added to the microwells and incubated for 20 min, which resulted in the development of a blue colour. The reaction was stopped by the addition of stopping solution, 1 N HCl, and the absorbance was measured spectrophotometrically at 450 nm (Sunrise™; Tecan, Switzerland). The absorbance measured was directly proportional to the concentration of hGH. The method was linear between 2.5 and 50 ng/ml. The LOD and LOQ were 0.5 and 1.5 ng/ml, respectively.

2.5. Visualising FITC-BSA deposition in P.L.E.A.S.E.® porated micropores using confocal laser scanning microscopy

Dermatomed porcine skin was porated using the P.L.E.A.S.E.® device (300 pores/cm^2 and 135 J/cm^2) and mounted in Franz diffusion cells. One ml of FITC-BSA solution (10 mg/ml) was placed in the donor compartment and kept in contact with the epidermal surface for 24 h. The receptor phase comprised of 10 ml Tris buffer (pH 7.4). At the end of the permeation experiment (24 h), the cells were dismantled and the skin was washed with 20% ethanol solution and gently dried with paper. The sample was then placed on a glass slide with the stratum corneum side up covered by distilled water. A cover slip was applied and FITC-BSA fluorescence was visualised as a function of depth within the skin using a Laser Scan Microscope 510 Meta (Carl Zeiss; Jena, Germany). The system was equipped with an Ar lamp laser (excitation lines at 488, 568, and 647 nm); FITC-BSA excitation and emission wavelengths were 488 and 520 nm, respectively. The confocal images were obtained with an Achroplan 20 × objective and analysed using Zeiss LSM Image Browser software. Each image was the average of eight repeated scans.

2.6. Statistical analysis

Data were expressed as Mean ± SD. Outliers determined using the *Grubbs test* were discarded. Results were evaluated statistically using either analysis of variance (ANOVA followed by *Student Newman Keuls test*) or by a two-tailed *Student's t-test*. The level of significance was fixed at $\alpha = 0.05$.

3. Results and discussion

3.1. Demonstrating the feasibility of protein delivery across laser porated skin

As expected, control experiments showed that there was no protein penetration or permeation across intact (untreated) skin after 24 h. In contrast, both penetration into and permeation across dermatomed porcine skin were observed after fractional laser ablation (Table 1). Total delivery of Cyt c, hGH, FSH and FITC-BSA after 24 h was 48.2 ± 8.9, 8.1 ± 4.2, 0.2 ± 0.1 and 273.3 ± 30.6 μg/cm^2, respectively (protein transport is calculated using the formulation application area and not the total porated surface area).

Given that the protein formulations used for the transport experiments were at different concentrations, it was decided to compare permeability coefficients estimated from the amount permeated (k_p) and the total delivery (sum of the amounts permeated and deposited in the skin; $k_{p,app}$) and these are shown in Fig. 2. The values of k_p for Cyt c, hGH, FSH and FITC-BSA were (1.6 ± 0.3), (0.1 ± 0.05), (0.08 ± 0.03) and (0.9 ± 0.1) × 10^{-3} cm/h, respectively. The values can be multiplied by a correction factor to take into account the fractional ablated area (FAA) and so obtain a permeability coefficient for transit through the microporated (or fractionally ablated) surface; given that the FAA was 7.22%, the correction factor is 13.85 and the 'corrected' k_p values are (22.2 ± 4.7), (1.4 ± 0.5), (1.2 ± 0.5) and (12.8 ± 1.7) × 10^{-3} cm/h, respectively. The estimated permeability coefficient for Cyt c was ~20-fold higher than those of hGH and FSH, which have only ~1.8- and 2.5-fold higher molecular weight. Surprisingly, the permeability coefficient of FITC-BSA was 10-fold higher than those of hGH and FSH despite its much higher molecular weight. It is clear that there was no simple correlation between the permeability coefficient of a protein for transit through the micropores and its molecular weight.

The dimensions of the micropores mean that there is little risk of steric hindrance to protein diffusion; hence, molecular weight and, implicitly, molecular volume are not limiting factors. It is more likely that the physicochemical properties of exposed amino acid residues at the protein surface or carbohydrate moieties introduced by post-translational modification (e.g. in FSH) have a significant influence on transport since they will determine the propensity of the protein to interact with the ablated skin or residual tissue in the microchannel during transit (see below). These surface-exposed amino acids and modifications determine protein–protein interactions and play a key role in biological function; thus, it is logical that they should also affect transport by controlling interactions with the local microenvironment.

Further insight into the differences in skin interaction potential of proteins can be gained by comparing results from skin deposition studies with Cyt c and FITC-BSA using dermatomed (750 μm; DS) and full thickness (1.5 mm; FTS) porcine skin. Although there was no statistically significant difference for Cyt c (9.3 ± 3.7 and 8.6 ± 4.5 μg/cm^2 for DS and FTS, respectively), skin retention of FITC-BSA was 3.5-fold higher in FTS (49.3 ± 8.3 and 172.1 ± 25.2 μg/cm^2 for DS and FTS, respectively). Thus, in the case

Table 1
Protein delivery as a function of ablation parameters and concentration.

Transport across DS			Cytochrome c				Human Growth Hormone				Follicle Stimulating Hormone				FITC-Bovine Serum Albumin			
			P[a] (μg/cm^2)	D[b] (μg/cm^2)	TD[c] (μg/cm^2)	Eff[d] (%)	P (μg/cm^2)	D (μg/cm^2)	TD (μg/cm^2)	Eff (%)	P (μg/cm^2)	D (μg/cm^2)	TD (μg/cm^2)	Eff (%)	P (μg/cm^2)	D (μg/cm^2)	TD (μg/cm^2)	Eff (%)
			38.8[e](8.1)[f]	9.4 (3.7)	48.2 (8.9)	14.5	8.1 (4.2)	–	8.1 (4.2)	0.5	0.05 (0.02)	0.1 (0.1)	0.2 (0.1)	2.3	222.2 (29.4)	49.3 (8.3)	271.5 (30.6)	8.1
Effect of pore number																		
Pore no.[g]	*Pore density (no./cm^2)*[h]	*FAA*[i] *(%)*																
0	0	0	–	–	–	–	–	–	–	–	–	–	–	–	–	–	–	–
150	50	1.20	–	–	–	–									58.5 (15.3)	21.2 (2.2)	79.7 (15.5)	2.4
300	100	2.41	11.2 (2.4)	11.3 (5.3)	22.5 (5.8)	6.7									132.6 (40.0)	43.2 (1.2)	175.8 (40.0)	5.3
450	150	3.61	15.3 (11.8)	3.5 (0.6)	18.8 (11.8)	5.6									192.7 (24.4)	42.3 (7.1)	235.0 (25.6)	7.1
900	300	7.22	33.9 (10.6)	9.6 (2.2)	43.3 (10.8)	13.1									293.4 (76.6)	45.1 (9.3)	338.5 (77.1)	10.2
1800	600	14.43	51.2 (15.8)	4.8 (2.4)	56.0 (16.0)	16.8									–	–	–	–
Effect of pore depth																		
Pulse no[j]	*Fluence*[k] *(J/cm^2)*	*FAA*																
5	22.65	7.22	33.9 (10.6)	9.6 (2.3)	43.5 (10.8)	13.1									53.4 (22.6)	16.5 (4.7)	69.8 (23.0)	2.1
10	45.3	7.22	48.5 (9.7)	8.4 (8.2)	55.2 (12.7)	16.6									293.4 (76.6)	45.1 (9.3)	338.5 (77.1)	10.2
20	90.6	7.22	28.9 (7.1)	9.9 (0.9)	38.8 (7.2)	11.6									329.6 (11.6)	63.3 (11.0)	393.0 (15.9)	11.8
30	135.9	7.22	38.8 (8.1)	9.3 (3.7)	48.1 (8.9)	14.4									218.2 (30.0)	49.3 (8.3)	267.5 (30.9)	8.0
Effect of protein conc. (mg/ml)																		
	1		33.9 (10.6)	9.6 (2.3)	43.5 (10.8)	13.1												
	5		295.4 (42.9)	32.3 (5.4)	327.7 (43.2)	19.7												
	0.025										0.05 (0.02)	0.1 (0.1)	0.2 (0.1)	2.3				
	0.165										0.8 (0.2)	0.9 (0.3)	1.7 (0.4)	3.1				
	0.33										0.7 (0.4)	1.4 (0.7)	2.1 (0.7)	1.9				
	0.66										2.0 (0.4)	2.2 (0.2)	4.4 (0.5)	2.0				

[a] P is the permeation across the skin after 24 h.
[b] D is the deposition within the skin after 24 h.
[c] TD is the total delivery, the sum of the amounts permeated and deposited after 24 h.
[d] Eff is delivery efficiency, the fraction of the amount applied that was delivered after 24 h.
[e] Mean value.
[f] Standard deviation is given in parentheses.
[g] Pore no. is the total number of pores created in the 3 cm^2 formulation application area.
[h] Pore density gives the number of pores created per unit area.
[i] FFA is the fractional ablated surface area.
[j] Pulse no. is the number of energy pulses applied to create the pore.
[k] Fluence is defined as the energy applied per pulse divided by the average pore area.

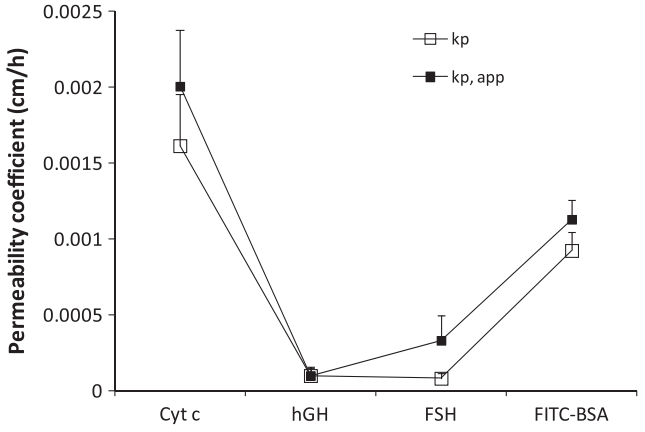

Fig. 2. Estimated permeability coefficients for Cyt c, hGH, FSH and FITC-BSA based on the amounts permeated (k_p) and the sum of the amounts permeated and deposited within the membrane ($k_{p,app}$); these are calculated based on the formulation application area and not the total ablated area of the skin surface (see text). The permeability coefficients for transport through the ablated surface area can be obtained by multiplication with a correction factor (13.85). Experiments performed using 900 pores (pore density 300 pores/cm^2, calculated from the number of pores divided by the application area, 3 cm^2) and at a fluence of 135 J/cm^2.

of Cyt c, there were a limited number of interaction sites in the epidermis and upper dermis and once these were occupied, there was no effect of increasing skin thickness. However, this was not the case for FITC-BSA, where use of FTS resulted in the provision of more interactions sites and consequently more skin retention of the protein.

The estimated permeability coefficients calculated here (k_p) are of the same order of magnitude as those observed for the low molecular weight drugs, diclofenac (296.1 Da) and granisetron (312.4 Da), across RF-treated porcine skin were 2.3×10^{-3} and 4.2×10^{-3} cm/h, respectively [30]. It should be noted that the latter study involved poration at a lower pore density and created smaller pores (100 pores/cm^2, with a total porated area of 2.8×10^{-3} cm^2 which corresponded to a fractional ablated area of 0.28%).

Delivery of hGH across porcine skin was extremely low (8.1 ± 4.2 μg/cm^2) with only ~0.5% of the applied amount permeating across or being recovered from the skin. This was in contrast to the reports on hGH delivery across rat and guinea pig skin using RF-induced stratum corneum ablation, where bioavailabilities of up to ~70 % and ~30 % (as compared to subcutaneous injection; 50 μg) were reported for the two animal models [7]. Those studies used dry patch formulations, where hGH was dissolved *in situ* by fluid released from the skin after microporation, resulting in high local protein concentrations that favoured transport. However, the skin of both rodents is known to be more permeable than human (or porcine) skin with respect to both passive and active delivery technologies, and these results may have overestimated the feasibility of hGH delivery.

The permeability coefficient for FSH transport was also low. Delivery of this protein may be affected by glycosylation since the presence of hydroxyl groups may facilitate interactions with the transport pathway through the formation of hydrogen bonds. It is well known that the presence of hydrogen bonds hinders diffusion across biological membranes.

Skin transport of FITC-BSA was quantified by using fluorescence spectroscopy to measure the intensity of fluorescence due to FITC. Mass spectrometric analysis of FITC-BSA samples post-delivery (i.e. recovered from the receiver compartment or from the skin itself) was undertaken in order to establish that the observed response was from FITC conjugated to BSA and not due to free FITC. In the mass spectra of FITC standard, the molecular ion peak for FITC was detected at m/z = 390.0. No such peak was detected in either the FITC-BSA standard or FITC-BSA skin permeation samples. Furthermore, the mass spectra for the FITC-BSA standard and the FITC-BSA samples post-delivery were identical. Thus, the mass spectrometric analysis confirmed that the fluorescence observed post-delivery was due to FITC conjugated to BSA and that it was possible to deliver hundreds of microgrammes of a ~70 kDa protein in 24 h. P.L.E.A.S.E.® poration followed by application of FITC-BSA solution in the donor compartment resulted in the labelling of the micropores (Fig. 3). Images of a single micropore in the XY- and XZ-planes are shown in Fig. 3b and c respectively; cylindrical pores with diameter ~150 μm and depth ~50 μm were observed following P.L.E.A.S.E.® poration.

3.2. Effect of pore density

Increasing the number of pores per unit area in the skin (i.e. the pore density) results in the formation of more molecular transport channels and should, in principle, increase delivery and indeed a statistically significant increase in cumulative skin permeation of Cyt c after 24 h was observed upon increasing pore density from 100 to 600 pores/cm^2 (ANOVA; F (12.6) > F_{crit} (3.28), $P = 2.2 \times 10^{-4}$) (Table 1 and Fig. 4a). Furthermore, cumulative permeation of Cyt c was linearly dependent on pore density (r^2 = 0.94) (Fig. 4b). Although there was no proportionate increase in skin deposition as a function of pore density, there was nevertheless a statistically significant increase in total delivery (permeation and deposition) of Cyt c upon increasing pore density from 100 to 600 pore/cm^2 (ANOVA; F (11.6) > F_{crit} (3.28), $P = 4.4 \times 10^{-4}$). At the highest pore density, which corresponded to a fractional ablated area of 14.43%, approximately 17% of the applied amount of Cyt c was delivered across P.L.E.A.S.E.® porated skin using a fluence of 22.65 J/cm^2 (which corresponds to shallow pores and thereby avoids damage to viable dermis [10]). Under these conditions, cumulative permeation after 24 h was 51.2 ± 15.8 μg/cm^2 (Table 1).

For comparison, cumulative iontophoretic delivery of Cyt c across dermatomed porcine skin at a current of 0.5 mA/cm^2 applied for 8 h to a 4.3 mg/ml Cyt c formulation was 923 ± 496 μg/cm^2 [31]. Thus, although fractional ablation of the stratum corneum and part of the viable epidermis was sufficient to enable passive diffusion along a concentration gradient across the skin, protein transport was less than that observed by using a second driving force, the potential gradient. It is possible that a combination of fractional laser ablation followed by electrically-assisted passage of charged molecules across the hydrophilic epidermis and dermis may enhance the rate and extent of macromolecular delivery.

Cumulative permeation of FITC-BSA also increased linearly with pore density (ANOVA; F (18.39) > F_{crit} (3.58), $P = 1.3 \times 10^{-4}$, r^2 = 0.92) (Fig. 5). Although there was a statistically significant increase in skin deposition of FITC-BSA on increasing pore density from 50 to 100 pores/cm^2, no further increase in the amount of FIC-BSA retained by the membrane was observed at higher pore densities. Total delivery increased as a function of pore density (ANOVA; F (20.2) > F_{crit} (3.58), $P = 8.7 \times 10^{-5}$); at a pore density of 300 pores/cm^2 with pores created using a fluence of 45.3 J/cm^2, approximately 10% of the applied amount of FITC-BSA was delivered across P.L.E.A.S.E.® porated skin.

These results are in good agreement with the observations from investigations into the effect of pore density on the delivery of lidocaine, prednisolone and diclofenac [10,12,14]. The presence of a linear correlation between cumulative permeation of Cyt c and FITC-BSA and pore density demonstrates that the number of microchannels per unit area and hence the fractional ablation area can be used to control macromolecule transport and hence the dose of a therapeutic protein that is delivered across the skin.

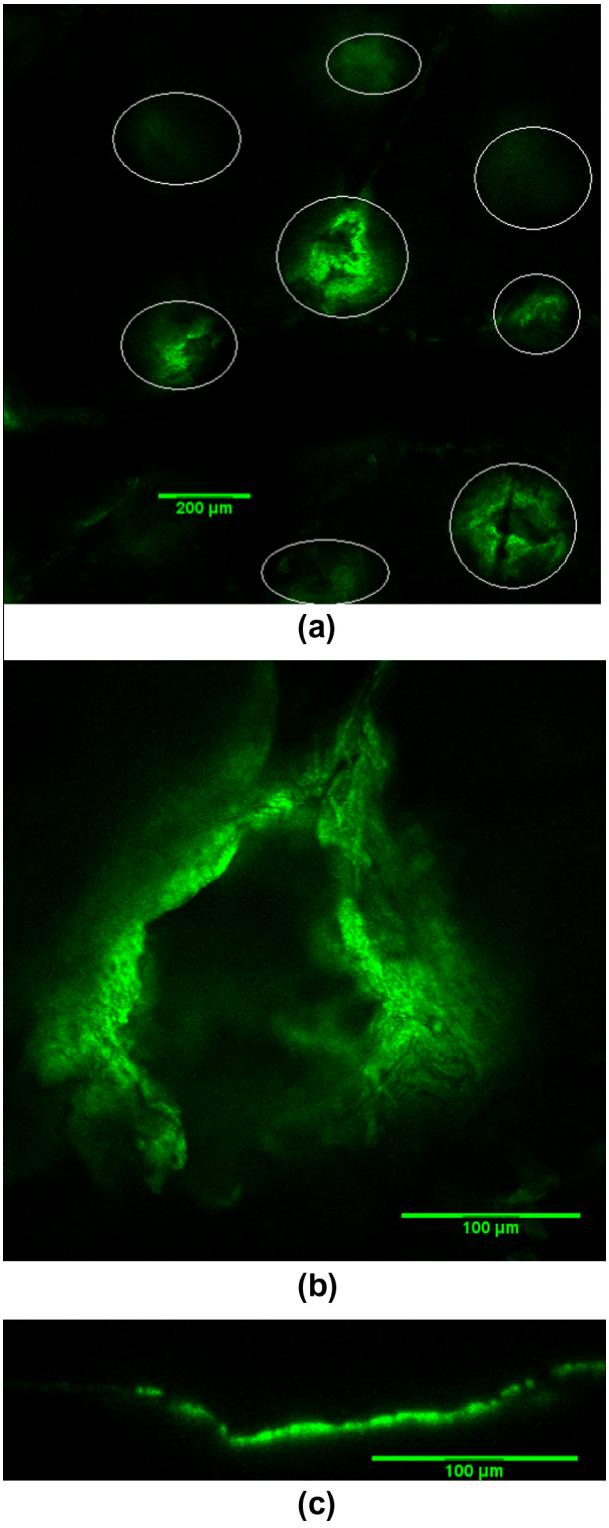

Fig. 3. Confocal laser scanning microscopy images of FITC-BSA across porcine skin following P.L.E.A.S.E.® poration; (a) group of micropores in the XY plane, (b) XY plane image of a micropore, (c) XZ plane image of micropore. (For interpretation of the references to colour in this figure legend, the reader is referred to the web version of this article.)

3.3. Effect of fluence

Fluence is defined as the laser energy applied per unit area to create each micropore. Histology studies of P.L.E.A.S.E.® porated porcine skin samples have revealed that the increase in fluence

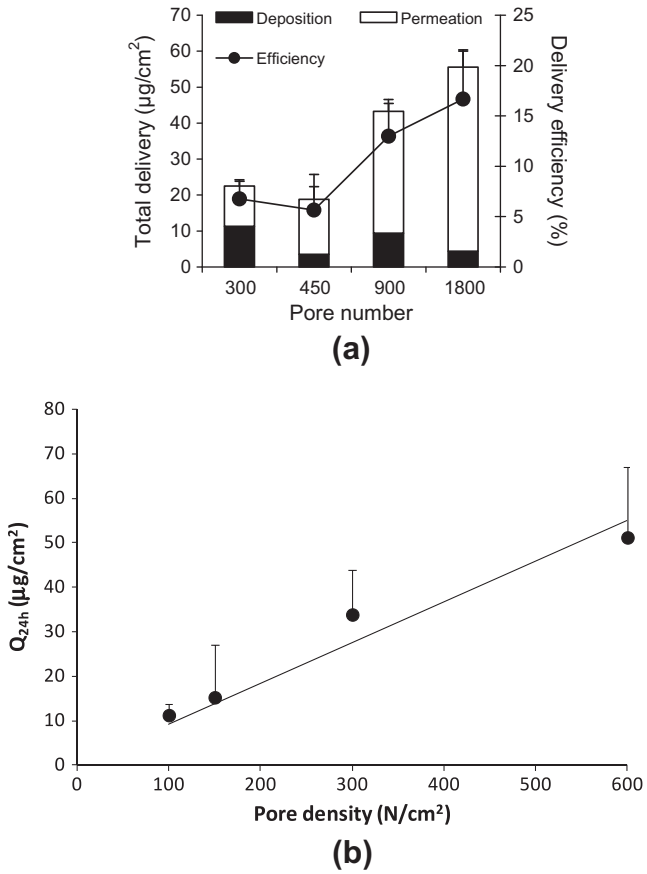

Fig. 4. (a) Effect of pore number on total delivery (sum of cumulative permeation and deposition) in 24 h and delivery efficiency of Cyt c and (b) the correlation between cumulative permeation (Q_{24h}) and pore density (calculated from the number of pores divided by the application area, 3 cm^2). Experiments were performed using a fluence of 22.65 J/cm^2 (Mean ± SD; n = 4–6).

leads to the formation of deeper pores and typical pore depths are around 50, 100, 150 and 250 µm at 22.65, 45.3, 90.6 and 135.9 J/cm^2, respectively [10]. Increase in fluence and thereby pore depth reduces the diffusional pathlength that the molecule must travel to cross the skin and the distance travelled through intact epidermis/dermis. Hence, it might be hypothesised that transdermal delivery should increase as a function of fluence. Thus, it was extremely surprising to observe that increasing fluence had no statistically significant effect on the total delivery of Cyt c (ANOVA; F (2.62) < F_{crit} (3.28), P = 0.08) (Fig. 6a). The absence of any dependence of Cyt c delivery on fluence (and hence pore depth) indicates that significant amounts of protein can be delivered by using shallower pores; hence, reducing the risk of irritation and 'damage' to the vascular dermis.

In contrast, increase in fluence had a clear statistically significant effect on total delivery of FITC-BSA (ANOVA, F (33.6) > F_{crit} (3.58), $P = 7.8 \times 10^{-6}$); the total amounts delivered at 45.3, 90.6 and 135.9 J/cm^2 were 340.1 ± 77.1, 395.3 ± 16.1 and 273.3 ± 30.63 µg/cm^2 were 4- to 5-fold greater than those seen after application of pulses at 22.65 J/cm^2 (70.3 ± 23.0 µg/cm^2) (Fig. 6b). Thus, at a fluence of 45.3 cm^2, approximately 10% (~1 mg) of the applied amount of FITC-BSA was delivered in 24 h.

The stratum corneum is recognised as the principal barrier to molecular transport into the skin; hence, its ablation and the formation of transport channels that enable direct transit to the viable epidermis will facilitate delivery. However, the micropores that are created are not 'empty' and contain desiccated tissue after the loss

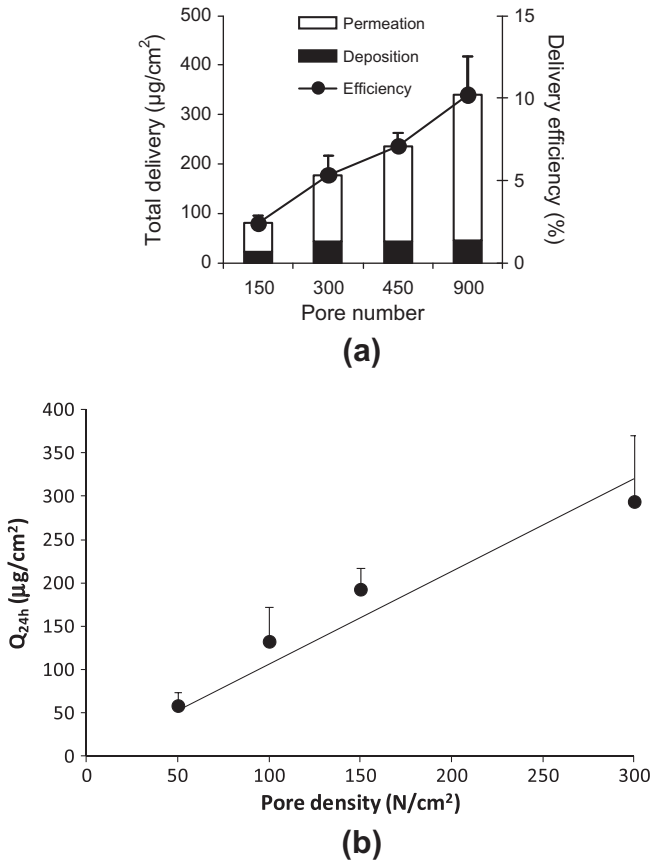

Fig. 5. (a) Effect of pore number on total delivery (sum of cumulative permeation and deposition) in 24 h and delivery efficiency of FITC-BSA and (b) the correlation between cumulative permeation (Q_{24h}) and pore density (calculated from the number of pores divided by the application area, 3 cm^2). Experiments were performed using a fluence of 45.3 J/cm^2 (Mean ± SD; n = 4–6).

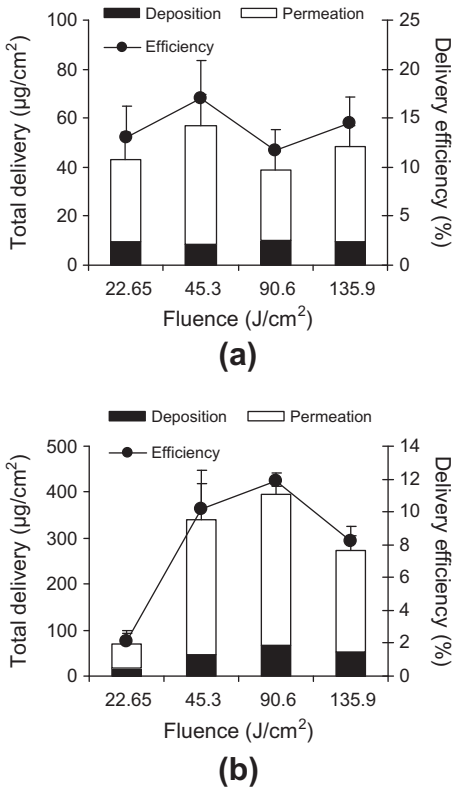

Fig. 6. Effect of fluence on total delivery (sum of cumulative permeation and deposition) in 24 h and delivery efficiency of (a) Cyt c and (b) FITC-BSA. The pore density was fixed at 300 pores/cm^2 (Mean ± SD; n = 4–6).

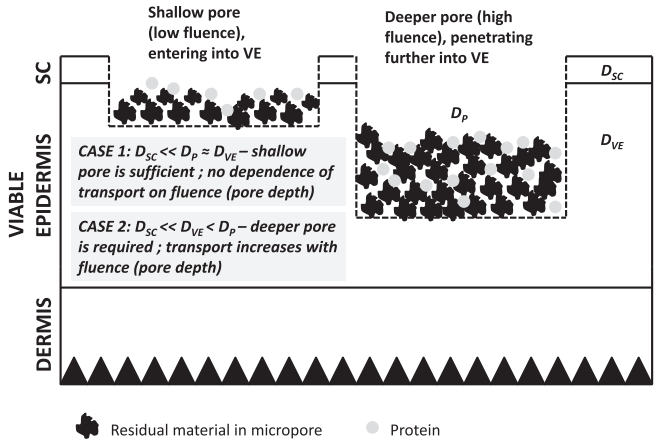

Fig. 7. The effect of fluence and hence pore depth on transport will be determined by the relative molecular diffusivities and interactions in the micropore as compared to those in 'bulk' non-porated epidermis/dermis. Given that the diffusivity in the SC, D_{SC} will be low, and then, after removal of the SC in the case of a molecule, where the diffusivities in the micropore (D_P) and viable epidermis (D_{VE}) are comparable, there is no benefit in using a higher fluence to create a deeper micropore (CASE 1). In contrast, if a molecule interacts strongly with epidermis, and $D_P > D_{VE}$, then there will be an increase in delivery as a function of fluence as the molecule permeates via the micropore rather than by diffusing through bulk tissue (CASE 2).

of epidermal water and will also fill with interstitial fluid *in vivo*. Thus, it is possible that any molecule in a micropore will interact with this local environment; the extent of the interaction will be determined by its physicochemical properties. These interactions are even more likely for complex biomolecules such as proteins with defined three dimensional structures, where regions of exposed surface will have hydrophilic or hydrophobic character and may interact with the micropores through van der Waals', electrostatic or hydrogen bond formation.

The effect of fluence and pore depth on transport will be determined by the relative molecular diffusivities and interactions in the micropore as compared to those in 'bulk' non-porated epidermis/dermis (Fig. 7). Hence, for a molecule, where the diffusivities in the micropore (D_P) and viable epidermis (D_{VE}) are comparable, there is no advantage in using a higher fluence to create a deeper micropore once the stratum corneum has been removed (CASE 1). In contrast, if a molecule interacts strongly with epidermis, and $D_P > D_{VE}$, then there will be an increase in delivery as a function of fluence as the molecule permeates via the micropore rather than by diffusing through bulk tissue (CASE 2). Cyt c belongs to the first category, and once the stratum corneum has been removed, there is no additional benefit in using a higher fluence to create deeper pores to facilitate molecular diffusion (Fig. 7). In contrast, we have previously shown that diclofenac delivery shows an extremely strong dependence on fluence and it can be deduced that it must interact with the membrane and hence the presence of deeper pores reduces this interaction and facilitates delivery [14]. FITC-BSA displays intermediate behaviour since increasing fluence from 22.65 to 45.3 J/cm^2 produced a ~5-fold improvement in delivery but further increases to 90.6 and 135.9 J/cm^2 did not produce any statistically significant effect.

3.4. Effect of donor concentration

Molecular transport through the micropores is by passive diffusion and is hence dependent upon the concentration gradient.

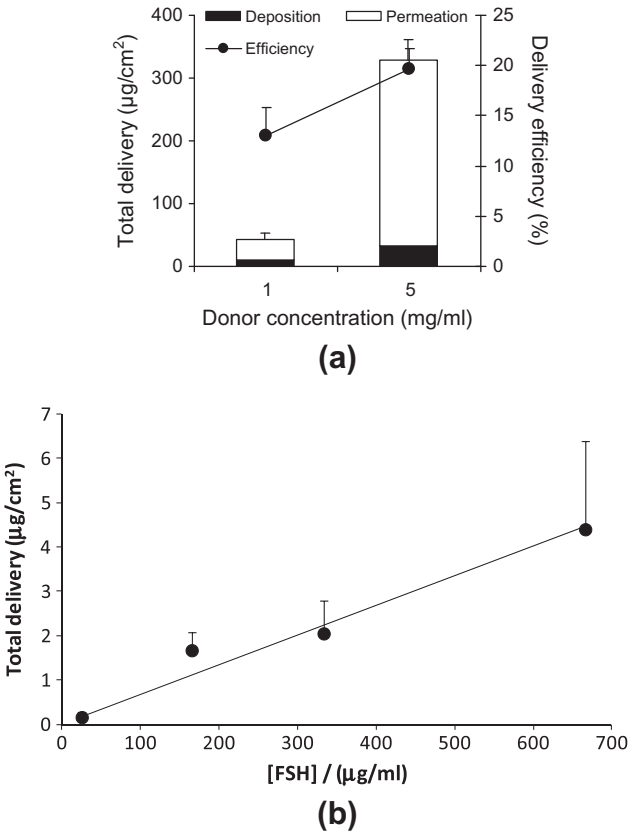

Fig. 8. Effect of protein concentration on total delivery (sum of cumulative permeation and deposition) in 24 h and delivery efficiency of (a) Cyt c and (b) FSH. In both cases, the pore density was 300 pores/cm^2 and the fluence was fixed at135 J/cm^2 (Mean ± SD; n = 4–6).

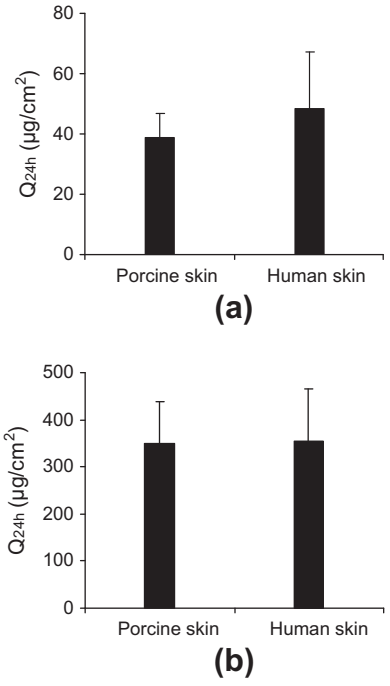

Fig. 9. Cumulative permeation (Q_{24h}) of (a) Cyt c and (b) FITC-BSA through P.L.E.A.S.E.® porated porcine and human skin in 24 h was statistically equivalent. Experiments performed at a pore density of 300 pores/cm^2 (or 900 pores in 3 cm^2) and a fluence of 135.9 J/cm^2 (Mean ± SD; n = 5–6).

Previous studies investigating the effect of concentration on lidocaine delivery across laser porated skin demonstrated that a 2.5-fold increase from 10 to 25 mg/ml produced a proportional increase in cumulative permeation after 24 h (1.65 ± 0.44 and 4.01 ± 1.39 mg/cm^2, respectively) [10]. Increasing the Cyt c concentration in the formulation from 1 to 5 mg/ml resulted in a ~9-fold increase in cumulative permeation (33.8 ± 9.4 and 295.3 ± 32.3 µg/cm^2, respectively) (Fig. 8a). This was accompanied by an approximately 7-fold increase in skin deposition (4.8 ± 2.4 and 32.3 ± 5.4 µg/cm^2, respectively). FSH delivery was also shown to increase with concentration; total delivery was 1.67 ± 0.36, 2.05 ± 0.74 and 4.40 ± 0.50 µg/cm^2 at 165, 330 and 666 µg/ml, respectively (cf. 0.16 ± 0.12 µg/cm^2 for 25 µg/ml) (Fig. 8b). Although the delivery efficiency observed in these preliminary studies with FSH was modest (~2–3%) (Table 1), nevertheless the amount of FSH delivered using the highest formulation concentration was ~13 µg, which corresponded to the lower limit of the therapeutic dose range administered daily by subcutaneous injection. These preliminary studies *in vitro* were the precursors to clinical trials that first demonstrated the feasibility of delivering FSH in human subjects and showed that the P.L.E.A.S.E.®- urinary FSH patch treatment was able to stimulate follicle growth and resulted in a successful pregnancy [16,32–34].

3.5. Comparison of transport kinetics across porcine and human skin

The final experiments compared cumulative permeation of Cyt c and FITC-BSA across P.L.E.A.S.E.® porated freshly excised human abdominal skin and porcine ear skin (900 pores, 135 J/cm^2). The results demonstrated that cumulative permeation of Cyt c across the two membranes was statistically equivalent (48.4 ± 18.8 and 38.8 ± 8.1 µg/cm^2; Student's test, α = 0.05) (Fig. 9a). Similar statistical equivalence was also observed for the cumulative permeation of FITC-BSA (355.5 ± 87.8 and 349.6 ± 109.7 µg/cm^2, for human and porcine skin, respectively; Student's test, α = 0.05) (Fig. 9b). The results confirmed the use of porcine ear skin as a good substitute for human skin for these *in vitro* experiments.

4. Conclusion

The results clearly demonstrate that laser microporation can be used for the controlled minimally invasive delivery of proteins into and across the skin. Moreover, transport rates can be modulated by variation of the micropore density (i.e. the fractional ablated area). They were also shown, in some cases, to depend on the fluence, that is, the pore depth. It was also observed that there was no simple relationship between protein delivery and molecular weight; it is proposed that the surface-exposed amino acids that govern interactions with the local microenvironment play a much more important role in determining transport than a crude descriptor such as molecular weight. This hypothesis obviously needs to be tested experimentally and will be investigated in future studies.

Acknowledgements

This work was supported by the Swiss Innovation Promotion Agency (CTI: 9307.1 PFLS-LS) and by Pantec Biosolutions AG. We would like to thank Dr. Kouroche Amini, Department of Plastic, Aesthetic and Reconstructive Surgery, Geneva University Hospital, for providing human skin samples. We would also like to acknowledge Dr. Christoph Bauer and Jerome Bosset of the Bioimaging Platform of the NCCR 'Frontiers in Genetics' at the University of Geneva for their help with confocal microscopy.

References

[1] B. Leader, Q.J. Boca, D.E. Golan, Protein therapeutics: a summary and pharmacological classification, Nat. Rev. Drug Discov. 7 (2008) 21–39.
[2] S. Frokjaer, D.E. Otzen, Protein drug stability: a formulation challenge, Nat. Rev. Drug Discov. 4 (2005) 298–306.
[3] A. Naik, Y.N. Kalia, R.H. Guy, Transdermal drug delivery: overcoming the skin's barrier function, Pharm. Sci. Technol. Today 3 (2000) 318–326.
[4] M.R. Prausntiz, S. Mitragotri, R. Langer, Current status and future potential of transdermal drug delivery, Nat. Rev. Drug Discov. 3 (2004) 115–124.
[5] Y.B. Schuetz, A. Naik, R.H. Guy, Y.N. Kalia, Emerging strategies for the transdermal delivery of peptide and protein drug, Expert Opin. Drug Deliv. 2 (2005) 533–548.
[6] M.R. Prausnitz, Microneedles for transdermal drug delivery, Adv. Drug Deliv. Rev. 56 (2004) 581–588.
[7] G. Levin, A. Gershonowitz, H. Sacks, M. Stern, A. Sherman, S. Rudaev, I. Zivin, M. Phillip, Transdermal delivery of human growth hormone through RF-microchannels, Pharm. Res. 22 (2005) 550–555.
[8] A.V. Badkar, A.M. Smith, J.A. Epstein, A.K. Banga, Transdermal delivery of interferon alpha-2B using microporation and iontophoresis in hairless rats, Pharm. Res. 24 (2007) 1389–1395.
[9] Y.N. Kalia, Y.G. Bachhav, T. Bragagna, C. Böhler, P.L.E.A.S.E.® (Painless Laser Epidermal System). A new laser microporation technology, Drug Deliv. Technol. 8 (2008) 26–31.
[10] Y.G. Bachhav, S. Summer, A. Heinrich, T. Bragagna, C. Böhler, Y.N. Kalia, Effect of controlled laser microporation on drug transport kinetics into and across the skin, J. Control. Release 146 (2010) 31–36.
[11] Y.G. Bachhav, Y.N. Kalia, Development and validation of an analytical method for the quantification of cytochrome c in skin transport studies, Biomed. Chromat. 24 (2010) 732–736.
[12] J. Yu, Y.G. Bachhav, S. Summer, A. Heinrich, T. Bragagna, C. Böhler, Y.N. Kalia, Using controlled laser-microporation to increase transdermal delivery of prednisone, J. Control. Release 148 (2010) e71–e73.
[13] Y.G. Bachhav, Y.N. Kalia, Development and validation of a rapid high performance liquid chromatography method for the quantification of exenatide, Biomed. Chromatogr. 25 (2011) 838–842.
[14] Y.G. Bachhav, A. Heinrich, Y.N. Kalia, Using laser microporation to improve transdermal delivery of diclofenac: increasing bioavailability and the range of therapeutic applications, Eur. J. Pharm. Biopharm. 78 (2011) 408–414.
[15] J. Yu, D.R. Kalaria, Y.N. Kalia, Erbium:YAG fractional laser ablation for the percutaneous delivery of intact functional therapeutic antibodies, J. Control. Release 156 (2011) 53–59.
[16] M. Zech NH, P. Uher, Pregnancy after ovarian superovulation by transdermal delivery of follicle-stimulating hormone, Fertil. Steril. 95 (2011) 2784–2785.
[17] R. Weiss, M. Hessenberger, S. Kitzmüller, D. Bach, E. Weinberger, W.D. Krautgartner, C. Hauser-Kronberger, B. Malissen, C. Boehler, Y.N. Kalia, J. Thalhamer, S. Scheiblhofer, Transcutaneous vaccination via laser microporation, J. Control. Release 162 (2012) 391–399.
[18] K.H. Wang, J.Y. Fang, C.H. Hu, W.R. Lee, Erbium:YAG laser pretreatment accelerates the response of Bowen's disease treated by topical 5-fluorouracil, Dermatol. Surg. 30 (2004) 441–445.
[19] J.Y. Fang, W.R. Lee, S.C. Shen, H.Y. Wang, C.L. Fang, C.H. Hu, Transdermal delivery of macromolecules by erbium:YAG laser, J. Control. Release 100 (2004) 75–85.
[20] W.R. Lee, S.C. Shen, C.R. Liu, C.L. Fang, C.H. Hu, J.Y. Fang, Erbium:YAG laser-mediated oligonucleotide and DNA delivery via the skin: an animal study, J. Control. Release 115 (2006) 344–353.
[21] W.R. Lee, T.L. Pan, P.W. Wang, R.Z. Zhuo, C.M. Huang, J.Y. Fang, Erbium:YAG laser enhances transdermal peptide delivery and skin vaccination, J. Control. Release 128 (2008) 200–208.
[22] M.H. Gold, Fractional technology: a review and clinical approaches, J. Drugs Dermatol. 6 (2007) 849–852.
[23] C.C. Dierickx, K.A. Khatri, Z.S. Tannous, J.J. Childs, R.H. Cohen, A. Erofeev, D. Tabatadze, I.V. Yaroslavsky, G.B. Altshuler, Micro-fractional ablative skin resurfacing with two novel erbium laser systems, Lasers Surg. Med. 40 (2008) 113–123.
[24] M.A. Trelles, S. Mordon, M. Velez, F. Urdiales, J.L. Levy, Results of fractional ablative facial skin resurfacing with the erbium:yttrium–aluminium–garnet laser 1 week a *d* 2 months after one single treatment in 30 patients, Lasers Med. Sci. 24 (2009) 186–194.
[25] B. Forster, A. Klein, R.M. Szeimies, T. Maisch, Penetration enhancement of two topical 5-aminolaevulinic acid formulations for photodynamic therapy by erbium:YAG laser ablation of the stratum corneum: continuous versus fractional ablation, Exp. Dermatol. 19 (2010) 806–812.
[26] G.W. Bushnell, G.V. Louie, G.D. Brayer, High-resolution three-dimensional structure of horse heart cytochrome c, J. Mol. Biol. 214 (1990) 585–595.
[27] L. Chantalat, N.D. Jones, F. Korber, J. Navaza, A.G. Pavlovsky, The crystal structure of wild-type growth hormone at 2.5 Angstrom resolution, Protein Pept. Lett. 2 (1995) 333–340.
[28] K.M. Fox, J.A. Dias, P. Van Roey, Three dimensional structure of human follicle-stimulating hormone, Mol. Endocrinol. 15 (2001) 378–389.
[29] K.A. Majorek, P.J. Porebski, M. Chruzcz, S.C. Almo, W. Minor, Crystal structure of bovine serum albumin. http://dx.doi.org/10.2210/pdb3v03/pdb <http://www.rcsb.org>.
[30] A.C. Sintov, I. Krymberk, D. Daniel, T. Hannan, Z. Sohn, G. Levin, Radiofrequency-driven skin microchanneling as a new way for electrically-assisted delivery of hydrophilic drugs, J. Control. Release 89 (2003) 311–320.
[31] J. Cazares-Delgadillo, A. Naik, A. Ganem-Rondero, D. Quintanar-Guerrero, Y.N. Kalia, Transdermal delivery of cytochrome c – a 12.4 kDa protein – across intact skin by constant–current Iontophoresis, Pharm. Res. 24 (2007) 1360–1368.
[32] Press release Announcing Results of Clinical Trial into the Use of P.L.E.A.S.E.® for the Transdermal Delivery of Follicle Stimulating Hormone, February 24, 2010. <http://www.pantec-biosolutions.com/en/events-and-news/press-releases/archive/pantec-biosolutions-reports-successful-phase-i-for-delivery-of-fsh-using-please> [Accessed 20.06.12].
[33] Press Release Announcing Clinical Efficacy Proof-of-Concept for Delivery of Urinary FSH Using P.L.E.A.S.E.®, December 15, 2010. <http://www.pantec-biosolutions.com/en/events-and-news/press-releases/archive/pantec-biosolutions-achieves-clinical-efficacy-poc-for-delivery-of-urinary-fsh-using-please> [Accessed 20.06.12].
[34] Press Release Announcing First Successful IVF Pregnancy Using P.L.E.A.S.E.® Patch, February 7, 2011. <http://www.pantec-biosolutions.com/en/events-and-news/press-releases/pantec-biosolutions-reports-first-successful-ivf-pregnancy-using-please-fsh-patch> [Accessed 20.06.12].